International Journal of Fracture (2006) 139:129–136
DOI 10.1007/s10704-006-8370-9

ON THE POSSIBILITY OF APPROXIMATION OF IRREGULAR POROUS MICROSTRUCTURE BY ISOLATED SPHEROIDAL PORES

Oleg Prokopiev and Igor Sevostianov
Department of Mechanical Engineering,
New Mexico State University, Las Cruces, NM 88001, USA
e-mail: igor@me.nmsu.edu

Abstract. Calculation of the effective elastic constants of a material with irregularly shaped porous space is discussed. It is shown that isolated pores of irregular shapes may be approximated, with good accuracy, by the spheroidal ones. Procedure of evaluation of the average aspect ratio from the photomicrograph is described. Several commonly used approximate schemes are applied to predict effective Young's and shear moduli of a material with spheroidal pores. Comparisons of these predictions with the experimentally measured elastic constants for completely sintered hydroxyapatite exhibit reasonably good accuracy. The best agreement is given by self-consistent and effective field methods.

1. Introduction. We discuss some aspects of the general problem of quantitative characterization of microstructures, which means identification of the *proper microstructural parameters*, in whose terms the effective elastic constants are to be expressed (Kachanov and Sevostianov, 2005). The key requirement is that these parameters should represent microstructural features in accordance with their actual contributions to the elastic constants; otherwise, they may not be unique functions of these parameters. For a material that can be described as continuous matrix with inhomogeneities (cracks, pores, inclusions), such parameters should characterize the distribution of inhomogeneities over shapes and orientations.

In most materials science applications, quantitative characterization of microstructures is complicated by their irregular character (inhomogeneities have complex irregular shapes) and insufficient information on the microgeometry (two-dimensional images). The latter problem has been addressed in a number of publications during last 20 years. Some rigorous closed-form relations between three-dimensional microstructures and their 2-D images were developed for several specific classes of inhomogeneities of particular shapes (see the book of Russ and Dehoff, 2000 for review). On the other hand, a number of various empiric shape factors are used in literature (see review in Kibbel and Heuer, 1989).

A simple method of determination of the microstructural parameters was suggested by Kibbel and Heuer, (1989) and Laraia *et al* (1994) for materials with inhomogeneities of spheroidal shape. In the present paper, we apply this approach to microstructures formed by pores of highly irregular shape which

are typical, in particular, for sintered ceramics. In particular, the hypothesis examined here can be formulated as follows:

> For calculation of the effective elastic constants of a material containing randomly oriented isolated pores of *irregular* shapes, the latter may be approximated, with good accuracy, by spheroidal ones and spheroid aspect ratios can be evaluated from the photomicrographs.

Microstructures of several specimens sintered at different temperatures were analyzed with Scanning Electron Microscope. First, we approximate the pores observed on 2-D images of random planar sections of specimens by ellipses and calculate average aspect ratios for each image. Then, using results of Laraia *et al* (1994), we construct imaginary porous material containing isolated spheroidal pores of the aspect ratio corresponding to these ellipses. We calculate elastic moduli of this imaginary porous material according to several commonly used approximate schemes (non-interaction approximation, self-consistent and differential effective media methods, Mori-Tanaka and Kanaun-Levin effective field methods) and compare them with the ultrasonically measured elastic moduli of the real material.

2. Experimental procedure. The hydroxyapatite have been obtained by precipitation method mixing the solution of ammonia phosphate $(NH_4)_2 HPO_4$ and suspension of calcium hydroxide $Ca(OH)_2$. The precipitation has been dried and ground into the powder with particle sizes 60-80 nm. The powder has been compressed under 20 MPa into the cylindrical specimens with the relative densities of compressed specimens ρ/ρ_0 varied in the range 32-36% based on theoretical density of hydroxyapatite $\rho_0 = 3.156\,\mathrm{g/cm}^3$. The specimens have been sintered at various temperatures ranging from 1220 to$1350\,^0$C for 3 hours. Elastic constants of the specimens have been measured by ultrasonic technique. The specimens have been broken during the compression test and the images of shatter microstructures have been obtained by SEM.

3. Analysis of images. The SEM images of specimen's microstructure have been processed with AutoCAD software package. All the pores of irregular shape have been replaced by best fitting ellipse and their areas and aspect ratios were calculated. To avoid complications related to the representative volume size, only images containing at least hundred inhomogeneities (pores) have been chosen for analyses. This process is illustrated by Fig. 1 where photomicrographs of irregular porous microstructures and corresponding approximations by ellipses are given for three specimens sintered at various temperatures.

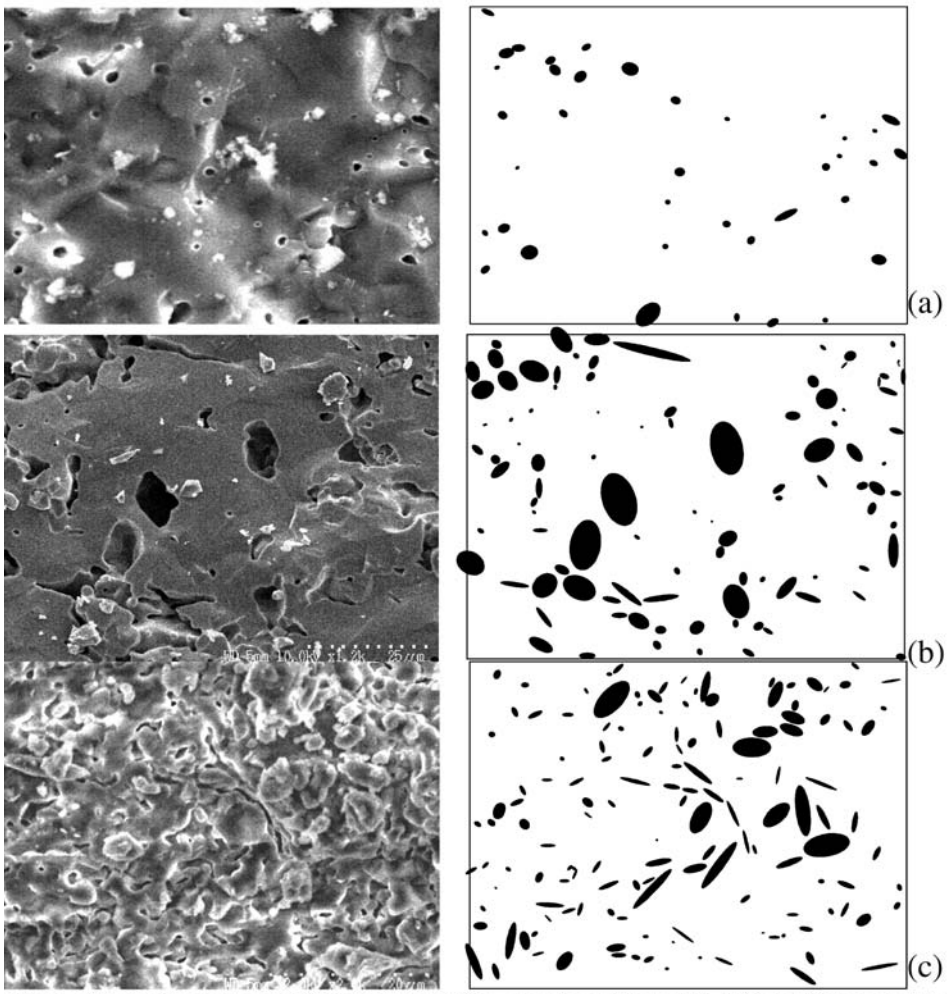

Fig 1. Microstructures and 2D models of the samples sintered at different temperatures: (a) 1350 °C, (b) 1320 °C, (c) 1220 °C

To construct approximations of microstructures, we utilize results of Laraia *et al* (1994) relating average aspect ratio of ellipses on random planar section and 3D spheroid aspect ratio. The authors employ area-weighted 2D shape factor:

$$R = \sum_i \frac{A_i \zeta_i}{A_T} \tag{3.1}$$

introduced by Kibbel and Heuer (1989), where ζ_i is 2D aspect ratio of *i*-th ellipse, A_i is its area and A_T is a total area occupied by ellipses in the random plane. In the case of oblate spheroids, their average aspect ratio according to Laraia *et al* (1994) is

$$\gamma = \frac{3}{2} R \tag{3.2}$$

The average values of γ for samples sintered at various temperatures are presented in Table 1. In the next section, we use these quantities to calculate elastic constants of a material containing randomly oriented spheroidal pores

Sintering temperature ^{C}C	Porosity	Densification rate (x10^{-4}) $\frac{\partial(\rho/\rho_0)}{\partial T}$	3D aspect ratio γ
1350	0.115	2.46	0.88
1340	0.129	2.99	0.87
1320	0.140	4.45	0.87
1280	0.143	9.81	0.98
1220	0.171	32.13	0.58

Table 1. Microstructural parameters for specimens sintered at various temperatures.

4. Calculation of the effective elastic properties. To calculate effective Young's and shear moduli of a material containing randomly oriented isolated spheroidal pores of aspect ratio γ (3.2), we apply several commonly used approximate schemes:

- Non-interaction approximation (see Kachanov *et al*, 1994)
- Self-consistent scheme (Skorohod, 1961; Hill, 1965)
- Differential scheme (McLaughlin, 1977; Zimmerman, 1991)
- Mori-Tanaka scheme (Mori and Tanaka, 1973; Benveniste, 1986)
- Kanaun-Levin's effective field method (Kanaun and Levin, 1994).

Predictions obtained by these methods are compared with the experimentally measured elastic constants of a material containing pores of irregular shape.

For randomly oriented spheroidal pores, all the mentioned schemes express the elastic moduli in terms of two parameters:

$$\alpha = \frac{(1+\nu_0)(54h_1 + 17h_2 + 52h_3 + 16h_5 + 14h_6)}{30} \tag{4.1}$$

$$\beta = \frac{2h_1 + 11h_2 - 4h_3 + 8h_5 + 2h_6}{30} \tag{4.2}$$

where coefficients

$$h_1 = \frac{(\kappa f_0 - f_1)}{2(4\kappa-1)\left[2(\kappa f_0 - f_1) - (4\kappa-1)f_0^2\right]};\ h_2 = \frac{1}{2[1-(2-\kappa)f_0 - f_1]};$$

$$h_3 = h_4 = \frac{-(2\kappa f_0 - f_0 + 2f_1)}{4(4\kappa-1)\left[2(\kappa f_0 - f_1) - (4\kappa-1)f_0^2\right]};$$

$$h_5 = \frac{1}{f_0 + 4f_1};\ h_6 = \frac{4\kappa - 1 - 6\kappa f_0 + 2f_0 - 2f}{4(4\kappa-1)\left[2(\kappa f_0 - f_1) - (4\kappa-1)f_0^2\right]} \tag{4.3}$$

are functions of the shape factors

$$f_0 = \frac{\gamma^2(1-g)}{2\left(\gamma^2-1\right)},\ f_1 = \frac{\kappa\gamma^2}{4\left(\gamma^2-1\right)^2}\left[\left(2\gamma^2+1\right)g-3\right] \tag{4.4}$$

Parameter g for oblate spheroids is

$$g = \frac{1}{\gamma\sqrt{1-\gamma^2}}\arctan\frac{\sqrt{1-\gamma^2}}{\gamma}, \tag{4.5}$$

where γ is spheroid's aspect ratio, and $\kappa = 1/(2-2\nu_0)$.

It is not the aim of the present paper to derive expressions for the effective elastic constants; see, for example, the review of Markov (2000). Below, we present the final formulas.

The effective Young's and shear moduli according to the non-interaction approximation are:

$$E = \frac{E_0}{1+p\alpha(\gamma,\nu_0)};\ G = \frac{G_0}{1+p\beta(\gamma,\nu_0)} \tag{4.6}$$

where functions $\alpha(\gamma,\nu_0)$ and $\beta(\gamma,\nu_0)$ are given by (4.1) and (4.2). The self-consistent scheme for the effective elastic constants leads to a system of two non-linear algebraic equations from which a single non-linear equation for Poisson's ratio can be obtained. Solving it leads to the following expressions for the effective Young's and shear moduli:

$$E = E_0(1-p\alpha(\gamma,\nu));\ G = G_0(1-p\beta(\gamma,\nu)) \tag{4.7}$$

Taking into account very weak dependence of parameters α and β on the Poisson's ratio (Sevostianov *et al*, 2006), one can use $\alpha(\gamma,\nu_0)$ and $\beta(\gamma,\nu_0)$ with accuracy better than 1%.

The differential scheme may be interpreted as the infinitesimal implementation of the self-consistent one. Thus, it leads to a system of two (differential) equations for elastic constants with obvious initial conditions $E\big|_{p=0} = E_0;\ G\big|_{p=0} = G_0$. Again, utilizing weak dependence of the parameters α and β on the Poisson's ratio, one gets

$$E = E_0(1-p)^{\alpha(\gamma,\nu_0)};\ G = G_0(1-p)^{\beta(\gamma,\nu_0)} \tag{4.8}$$

In contrast with the self-consistent and differential schemes, effective field method allows one to work with single equations rather than systems. In particular, Mori-Tanaka and Kanaun-Levin schemes give the following expressions for the effective Young's and shear moduli:

Mori-Tanaka scheme

$$E = \frac{E_0}{1+\dfrac{p}{1-p}\alpha(\gamma,\nu_0)} \qquad G = \frac{G_0}{1+\dfrac{p}{1-p}\beta(\gamma,\nu_0)} \tag{4.9}$$

Kanaun-Levin's method

$$E = \frac{E_0}{1 + \dfrac{p\alpha(\gamma,\nu_0)}{1 - p\,\alpha(\gamma,\nu_0)/\alpha(1,\nu_0)}}; \quad G = \frac{G_0}{1 + \dfrac{p\beta(\gamma,\nu_0)}{1 - p\,\beta(\gamma,\nu_0)/\beta(1,\nu_0)}} \qquad (4.10)$$

The values of the effective Young's and shear moduli predicted according to these schemes are given in Tables 2 and 3, respectively. Numbers in parentheses show the deviation from ultrasonically measured elastic constants of sintered hydroxyapatite with irregular porous microgeometry.

Table 2 Comparison of the experimentally measured Young's modulus of sintered hydroxyapatite with ones calculated by various approximate methods. Disagreement with experimental data is given in parenthesis

Sintering temp.	Experiment	Non-interaction approx.	Self-consistent scheme	Differential scheme	Mori-Tanaka scheme	Kanaun-Levin effective field method
°C	GPa	GPa	GPa	GPa	GPa	GPa
1350	78.2	86.3 (10.4%)	77.5 (0.9%)	81.1 (3.7%)	83.7 (7.0%)	83.7 (7.0%)
1340	73.5	83.8 (14.1%)	73.0 (0.7%)	77.6 (5.5%)	80.7 (9.8%)	80.7 (9.8%)
1320	67.3	82.0 (21.8%)	69.5 (3.2%)	74.9 (11.2%)	78.4 (16.5%)	78.4 (16.5%)
1280	59.8	81.6 (36.4%)	68.7 (14.8%)	74.2 (24.1%)	77.9 (30.2%)	77.9 (30.2%)
1220	41.6	76.1 (82.8%)	57.1 (37.3%)	66.0 (58.6%)	71.2 (71.1%)	70.9 (70.4%)

Table 3 Comparison of the experimentally measured shear modulus of sintered hydroxyapatite with ones calculated by various approximate methods. Disagreement with experiment data is given in parenthesis

Sintering temp.	Experiment	Non-interaction approx.	Self-consistent scheme	Differential scheme	Mori-Tanaka scheme	Kanaun-Levin effective field method
°C	GPa	GPa	GPa	GPa	GPa	GPa
1350	33	40.4 (9.4%)	34.9 (5.6%)	39.9 (20.8%)	33.0 (0.2%)	33.0 (0.2%)
1340	33.2	39.9 (9.1%)	33.6 (1.3%)	39.3 (18.2%)	31.8 (4.3%)	31.8 (4.3%)
1320	29.7	39.5 (14.6%)	32.7 (10.0%)	38.8 (30.5%)	30.9 (3.9%)	30.9 (3.9%)
1280	25.8	39.4 (22.8%)	32.4 (25.7%)	38.7 (49.8%)	30.7 (18.8%)	30.7 (18.8%)
1220	16.8	38.3 (51.6%)	29.4 (75.1%)	37.2 (121.1%)	28.0 (66.8%)	27.9 (66.1%)

5. Discussion. We examined the possibility to replace irregularly shaped porous space in sintered hydroxyapatite by isolated spheroidal pores in the process of calculation of the effective elastic properties. For the specimens processed at high temperatures (1320 ^{0}C and higher), calculated values of

Young's and shear moduli are in good agreement with the experimentally measured. For specimens sintered at lower temperatures, this approximation does not appear to be reasonable. The explanation of this observation can be obtained from the analysis of Figure 2, where ρ_0 and ρ are initial and sintered specimen density respectively (see Table 1). The rate of the mass transport $\frac{\partial(\rho/\rho_0)}{\partial T}$ (or *densification rate*) has been calculated for every temperature based on the fitting curve shown by dashed line. Low values of this parameter for the sintering temperatures 1320 ^{0}C and above refer to the final stage of sintering, i.e. complete sintering where density remains approximately constant and elastic properties are affected by only two counteracting phenomena: changing of the pore shapes and grain growth. Note that the factor of pore shape completely dominates over the effect of the grain growth (Prokopiev and Sevostianov, 2006).

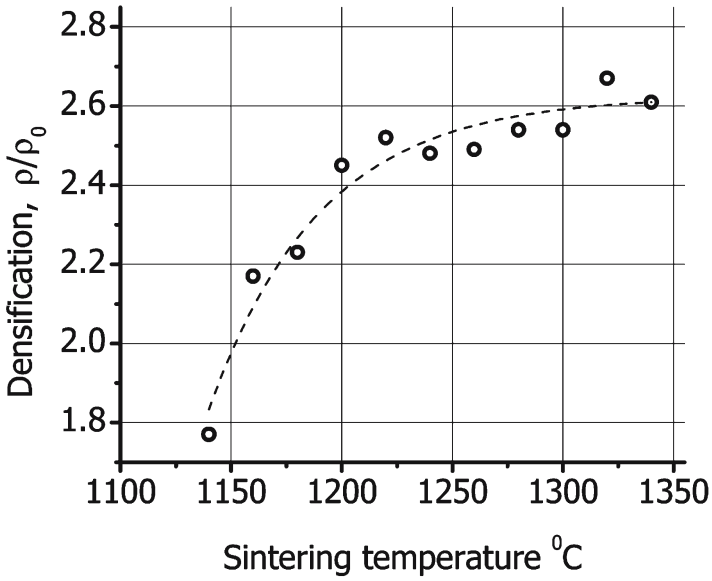

Figure 2. Relative density of specimens as a function of sintering temperature.

As illustrated by Fig 2, that densification rate for the specimens sintered at the 1220 ^{0}C is almost three times higher than for the specimens sintered at 1280 ^{0}C and more than seven times higher than for the specimens sintered at 1320^{0}C. It means that sintering temperature lower than 1280 ^{0}C is insufficient to produce completely sintered material during the sintering time used in the experiments. As a result, we obtained specimens with very complex morphology: mixture of pores of irregular shape and contacts between separate hydroxyapatite grains. Such a microstructure cannot be adequately represented by isolated pores embedded in a continuous matrix.

An interesting observation can be made from Tables 2 and 3 regarding various approximate schemes. All the examined methods predict results that are *higher* than experimentally measured - it is due to the well known fact that deviations from spherical shape increase pore compliance. The differential scheme gives the highest overestimation of the experimental data. Predictions according to Kanaun-Levin and Mori-Tanaka's schemes almost coincide. Young's modulus is better described by self-consistent scheme while the shear modulus is better predicted by Kanaun-Levin's scheme.

Remark. The results presented here are obtained for materials containing pores close to spherical ones. As seen from Table 1, the average aspect ratio of pores in completely sintered materials is higher than 0.85 (the case of randomly oriented slightly deformed spheres discussed by Kachanov *et al*, 1994). For this reason, we cannot evaluate the adequacy of the expression (3.1) for the average 2-D aspect ratio. It appears to be physically more reasonable to consider squares of the aspect ratios of individual ellipses. This problem is still open.

References:

Benveniste, Y. (1986) On the Mori-Tanaka's method in cracked bodies *Mechanics Research Communications*, 13(4), 193-201.

Hill, R. (1965). A self-consistent mechanics of composite materials. *Journal of the mechanics and physics of solids* 13(4), 213-222.

Kachanov, M. & Sevostianov, I. (2005). On quantitative characterization of microstructures and effective properties. *International Journal of Solids and Structures* **42**, 309-336.

Kachanov, M., Tsukrov, I. & Shafiro, B. (1994). Effective moduli of solids with cavities of various shapes. *Applied Mechanics Reviews*, 47(1), S151-74

Kanaun, S. & Levin, V. (1994). in: K. Markov (Ed.) Advances in Mathematical Modeling of Composite Materials, World Scientific, Singapore, p.1.

Kibbel, B. & Heuer, A. (1989) Anisometric shape factors for microstructures. *Journal of American Ceramic Society* , **72**, 517-19.

Laraia, V., Rus, I., & Heuer, A. (1994) Microstructural shape factors: relation of random planar section to three dimensional microstructures. *Journal of American Ceramic Society* 78(6) 1532-36.

Markov, K. (2000). in: Markov, K, Preziozi, L.(Eds.), Heterogeneous Media: Micromechanics Modeling Methods and Simulations, Birkhauser, Boston, p.1

McLaughlin, R. (1977). A study of the differential scheme for composite materials. *International Journal of Engineering Science.* 15(4), 237-44.

Mori, T. & Tanaka, K. (1973) Average stress in matrix and average elastic energy of materials with misfitting inclusions. *Acta Metallurgica,*21(5) 571-74

Prokopiev, O & Sevostianov, I. (2006) *Materials Science and Engineering A.* (In press)

Russ, C, & Dehoff. (2000). *Practical Stereology*, 2nd Edition, Plenum Press, NY.

Sevostianov, I., Kováčik, J. & Simančík. (2006). Elastic and electric properties of closed-cell aluminium foams Cross-property connection. *Materials Science and Engineering A.* 420 87-99, 2006.

Skorohod, V. (1961). Calculation of the effective isotropic moduli of disperse solid systems, *Poroshkovaja Metallurgija (Powder Metall.)* 1, 50-55. (in Russian).

Zimmerman, R. (1991). Elastic moduli of a solid containing spherical inclusions. *Mechanics of Materials.* 12(1), 17-24.